Magmatic Processes: Physicochemical Principles
© The Geochemical Society, Special Publication No. 1, 1987
Editor B. O. Mysen

Steady state double–diffusive convection in magma chambers heated from below

STEPHEN CLARK[1,2], FRANK J. SPERA[2] and DAVID A. YUEN[3]

1) Department of Geological and Geophysical Sciences, Princeton University, Princeton, NJ 08544 U.S.A.
2) Department of Geological Sciences, University of California, Santa Barbara, CA 93106 U.S.A.
3) Department of Geology, University of Minnesota, Minneapolis, MN 55455
and Minnesota Supercomputer Institute, University of Minnesota U.S.A.

Abstract—In order to deduce the vertical structure of doubly–diffusive convection cells in magma chambers, solutions to the horizontally–averaged conservation equations governing the distribution of temperature, composition and velocity in a two component (rhyolite–basalt) Newtonian melt have been obtained. Boundary conditions were chosen to model a chamber with a hot, dense (basaltic) base, overlain by cooler more silicic magma, where the influences of sidewall cooling, crystallization and melting are not considered. Parameters of the problem are: the Lewis number, a ratio of thermal to compositional diffusivities ($\mathrm{Le} \equiv \kappa/D$); the Prandtl number, a ratio of viscosity to thermal diffusivity ($\mathrm{Pr} \equiv \nu/\kappa$); the Rayleigh number, a ratio of thermal buoyancy to viscous forces ($\mathrm{Ra} \equiv \alpha g d^3 \Delta T/\kappa\nu$, where α is thermal expansivity, d is the magma chamber depth and ΔT the temperature difference across the chamber); the buoyancy ratio, a ratio of compositional to thermal buoyancy ($R\rho \equiv \alpha_C \Delta C/\alpha \Delta T$, where α_C is compositional expansivity and ΔC the compositional difference across the chamber); the ratio of maximum to minimum magma viscosities (Λ) and the wavenumber of convection (k).

Steady state solutions have been obtained for values of these parameters in the range appropriate to magma chambers and include the effects of a strongly temperature–dependent viscosity. Calculations show that a critical Lewis number ($\mathrm{Le}_{\mathrm{crit}}$) separates steady single–cell convection from unsteady convection and conduction. For isoviscous convection at a wavenumber $k = \pi$ and for $\mathrm{Le} > \mathrm{Le}_{\mathrm{crit}} = 6.7\ \mathrm{Ra}^{-0.12} R\rho^{1.67}$, single–layer convection cells characterized by thin chemical and thermal boundary layers and well–mixed interiors develop. Magma chambers lie above this critical Lewis number and, therefore, steady–state model magma chambers exhibit single cell convection. When a temperature dependent viscosity is assumed, the style of convection is not qualitatively different. Steady state values of the heat flux through the chamber roof and the flux of light component downward are given by $q = 0.4 k_T \Delta T d^{-1}\ \mathrm{Ra}^{0.23}\ \mathrm{Le}^{0.01} R\rho^{0.01} \Lambda^{0.10}$ and $j = 0.4 \kappa \Delta C d^{-1}\ \mathrm{Ra}^{0.23}\ \mathrm{Le}^{-0.65} R\rho^{0.01} \Lambda^{0.05}$, respectively, where k_T is the thermal conductivity. Calculated heat flow values in the range 2000 to 20 000 mW/m^2 compare favorably with measurements in active geothermal areas. Redistribution times for major elements by advective–diffusive transport are in the range 10^5 to 10^6 years. These redistribution rates indicate effective eddy diffusivities 10^5 to 10^6 times larger than Fickian chemical diffusivities. Maximum convection velocities are given by $W = 0.10 \kappa d^{-1}\ \mathrm{Ra}^{0.62}$, which implies maximum velocities in the range 1 to 10^2 km/year (far greater than crystal settling rates) for typical chambers. Crystal settling is therefore restricted to the chamber margins where convective velocities are much smaller. A difference in steady–state behavior is observed as the Prandtl number is lowered below twenty. It is suggested that effects of inertia can cause differences in the dynamic behaviour of double–diffusive convection.

For convection cell aspect ratios greater than about 3 (*i.e.*, cell 3 times deeper than wide) two steady state solutions are found. The solution corresponding to a high heat flux is a single layer (whole chamber) convection cell whereas the low heat flow solution consists of two vertically stacked convection cells separated by a thin diffusive interface. Similar layers are found in thermal convection experiments performed at high wavenumbers. Such layering must therefore be due to chamber geometry and not the influence of compositional buoyancy.

INTRODUCTION

NUMEROUS STRATIGRAPHIC STUDIES of individual pyroclastic flow deposits over the past 50 years have revealed the presence of discrete compositional gaps in major, minor and trace elements (*e.g.*, WILLIAMS, 1942; TSUYA, 1955; SMITH, 1960; LIPMAN, 1967; HILDRETH, 1981). For example, a 30 m thick ash flow tuff has been described from Gran Canaria, that consists of a single cooling unit with a rhyolitic base, a basaltic top and a thin (~2 m) mixed zone interior (SCHMINCKE, 1969; CRISP, 1984; CRISP and SPERA, 1986). Similarly, at Crater Lake, Oregon, USA, WILLIAMS (1942) described "the eruption of two magma types in rapid succession", a 66–69 weight percent SiO_2 dacitic and a 54–57 weight percent basic magma (see also BACON, 1983). In addition to cases where compositional gaps occur in vertical stratigraphic sections, many examples of mixed–pumice eruptions have been described (*e.g.*, Smith, 1979; Hildreth, 1981). In a mixed–pumice pyroclastic flow, two or more compositionally distinct magma types are simultaneously erupted from a single vent.

The mechanism(s) for generation of compositional gaps in ash flow deposits are not clear. Recently it has been shown that significant variations in discharge rate during an eruption can produce compositional gaps in deposits even if the *in situ* (pre–eruptive) chemical gradient is linear (Greer, 1986; Spera *et al.*, 1986a). That is, a compositional gap could be an artifact of the hydrodynamics of magma withdrawal. On the other hand, it has been suggested that layering may be the product of double–diffusive convection within magma chambers (McBirney, 1980; Turner, 1980; Rice, 1981; Huppert and Sparks, 1984). Two distinct models for magma chamber convection are illustrated in Figure 1. Double–diffusive convection exists when two scalars of differing molecular diffusivities, such as temperature and composition, contribute to the buoyancy of the fluid in opposing directions. Two types of double–diffusive convection may be distinguished. The first occurs when the fast diffusing 'component' (*i.e.,* heat) has an unstable distribution and is called the "diffusive regime". Layered convection may develop in this regime (Figure 1). The second regime occurs when the slow diffusing component has an unstable distribution. This regime is called the "finger regime" and is discussed at length by Schmitt (1979, 1983) and Piasek and Toomre (1980). In a crustal magma chamber, dense hot basic magma commonly underlies cooler silicic magma. Heat diffuses much faster than any chemical component in magmatic liquids, and, therefore, magma chambers are commonly in the "diffusive regime". The finger regime may also be relevant to magma chamber evolution. For instance, in a closed system chamber (*i.e.,* no replenishment) where crystallization can produce an iron–enriched liquid, a relatively dense iron-rich melt can come to lie above a cold stagnant bottom boundary layer (Jaupart *et al.,* 1984; Brandeis and Jaupart, 1986). In this paper, attention is focused on the diffusive regime because it is most relevant to the origin of compositional layering in pyroclastic flows. Exhumed layered intrusions, such as the Stillwater Complex in Montana, USA, present difficulties in interpretation because of the drastic compositional effects imposed by magma crystallization. Pyroclastic flows, on the other hand, are melt dominated often containing only 5 to 10 volume percent phenocrysts.

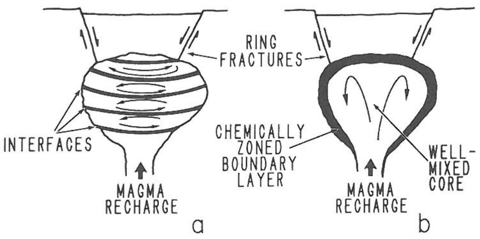

FIG. 1. Schematic depiction of (a) layered convection and (b) single–cell convection in a large volume magma chamber. In (a) distinct well–mixed and nearly isothermal regions are separated by thin diffusive interfaces characterized by steep gradients of composition and temperature. Case (b) represents single–cell convection occupying the whole magma chamber. The main body of the chamber is chemically homogeneous and isothermal. The only chemical and thermal zonation is restricted to thin boundary layers surrounding the chamber.

Previous work on double–diffusive convection (or more generally multiple–component convection) includes analytic, experimental and numerical studies (*e.g.,* Veronis, 1965; Baines and Gill, 1969; Proctor, 1981; Knobloch and Proctor, 1981; Da Costa *et al.,* 1981; Chen and Turner, 1980; Turner, 1980; Newell, 1984; Veronis, 1968; Elder, 1969; Huppert and Moore, 1976; Gough and Toomre, 1982; Moore *et al.,* 1983; Knobloch *et al.,* 1986). The recent summaries by Chen and Johnson (1984) and especially Turner (1985) provide comprehensive surveys of multicomponent convection from both historical and modern viewpoints.

The aim of this work is to carry out numerical experiments under a set of conditions applicable to magma chambers with the hope of discovering the nature of double–diffusive convection there. Of particular relevance to volcanologists and geochemists is the question of whether or not layered convection exists in magma reservoirs from which pyroclastic flows are erupted. In the present work, attention is focused on possible steady–state layered chambers. The details of flow development will be discussed later. The nature of multicomponent convection in the steady state is the logical starting point for any future studies aimed at the transient behavior of convection in magma reservoirs. A similar approach was taken by mantle convection workers who studied steady state solutions (Turcotte and Oxburgh, 1967) long before time–dependent solutions (McKenzie *et al.,* 1974). The present paper is an amplification of the preliminary study by Spera *et al.* (1986b).

ANALYSIS

Mean field approximation

The equations that govern the form of the velocity, temperature and compositional fields within a convecting magma body include the conservation of mass, linear momentum, energy and composition. Magma is treated as a binary fluid composed of a silicic (light) component and a complementary mafic (dense) component. The chemical properties of the light component enter into the equations only in terms of its molecular diffusivity (D) and a thermodynamic parameter (α_C) analogous to the isothermal expansivity. The α_{SiO_2} and α_{H_2O} in intermediate composition melts are roughly 0.3 and 2 respectively. Values of α_C are listed in Table 1.

In this study the single-mode mean field method has been utilized (HERRING, 1963). This method is able to exhibit both the basic physics of the convection and also the scaling relations between quantities such as heat flux and vigor of convection. This approach basically entails the *a priori* prescription of the size and form of the convection cells. This allows horizontal averaging of quantities such as velocity, and hence the dimensionality of the problem is reduced to one dimension; depth. In comparison with two-dimensional (2–D) methods the mean field approach is considerably cheaper; because of this it is possible to perform many experiments over a range of difficult conditions. We regard the mean field method as a reconnaissance tool which enables a better interpretation of two-dimensional (2–D) numerical simulations (OLDENBURG *et al.,* 1985, HANSEN and YUEN, 1985, HANSEN, 1986). This consideration is a primary motivation for the present study.

Calculations for the case of constant viscosity convection by QUARENI and YUEN (1984) have found good agreement between mean-field and 2–D results in both steady-state and time dependent situations. For variable viscosity thermal convection, an extensive study (QUARENI *et al.,* 1985), involving both temperature- and pressure-dependent rheologies, gave further support to the usage of the mean field for the purpose of obtaining scaling relations. For example the power-law exponents relating heat flux and the vigor of convection differ by at most 10% between mean field and 2–D methods. The recent findings of P. OLSON (1986) demonstrate the relationship between mean field, 2–D and boundary layer predictions. The essential features of the dependence of boundary-layer thicknesses upon the strength of convection is captured by both mean field and 2–D methods. More important is the finding that the 2–D results lie between those of the mean field and boundary-layer methods when heat transfer or boundary layer thicknesses are compared. Furthermore the ability of the mean field method to resolve internal interfaces is clearly demonstrated by the prediction of layered thermal convection in narrow slots. Such convection was also found in the experimental study of J. M. OLSON and ROSENBERGER (1979).

Table 1. Calculated values for the coefficient of isothermal chemical expansivity*

$$\alpha_C = -\rho^{-1}\left(\frac{\partial \rho}{\partial C}\right)_T$$

	Basaltic Magma	Rhyolitic Magma
SiO_2	+0.41	+0.22
TiO_2	−0.30	−0.43
Al_2O_3	−0.05	−0.08
Fe_2O_3	−0.28	−0.39
FeO	−0.62	−0.68
MnO	−0.47	−0.54
MgO	−0.20	−0.32
CaO	−0.21	−0.33
Na_2O	+0.25	+0.01
K_2O	+0.26	+0.05
H_2O	+3.00	+2.00

* Calculated from BOTTINGA *et al.* (1982). Reference density and temperature for basalt and rhyolite are 1200°C, 2.6738 g/cm^3 and 900°C, 2.2781 g/cm^3 respectively. Values for water derived from BURNHAM and DAVIS (1971).

When comparing two– and three-dimensional (3–D) studies workers (LIPPS and SOMERVILLE, 1971, and MCKENZIE *et al.,* 1974) have noted discrepancies. These discrepancies result from the fact that in a full 3–D model the convective planform wavelength is dependent on the vigor of convection, as measured by the Rayleigh number. If this dependence is known, and used in 2–D and mean field simulations, good results are obtained; frequently, however, it is not known. In our numerical experiments planform wavelength is fixed *a priori.* An estimate of the error incurred by this procedure can be obtained by performing a set of numerical experiments over a range of wavelengths. It is shown later that the error introduced is *at most* a factor of two in terms of predicted heat fluxes, convection rates and boundary layer thicknesses.

The inherent limitations of the mean-field approximation are overshadowed by our immense ignorance concerning the most basic features of magma chambers. For example geological and geophysical constraints on magma chamber geometries are meager (IYER, 1984), as are data on relevant rates of heat and mass transfer along chamber–country rock contacts. Furthermore, it is an experimental fact that magma is a rheologically complex fluid (SHAW, 1969; SPERA *et al.,* 1982; MURASE *et al.,* 1985) with a constitutive relation that changes as crystals nucleate and grow. In view of this incomplete understanding, we have chosen a canonical set of magma chamber properties. In particular we study large chambers heated from below, where the influence of sidewall cooling can be neglected. The role of various sidewall boundary conditions has been previously examined (*e.g.*, SPERA *et al.*, 1982; LOWELL, 1985; SPERA *et al.*, 1984; NILSON *et al.*, 1985; NILSON and BAER, 1982).

Conservation equations

The mean field equations are derived from the two–dimensional equations of conservation of momentum, energy and composition. Following VERONIS (1968) the Boussinesq equation of motion is,

$$\left(\frac{\partial}{\partial t}+v\cdot\nabla\right)v=\frac{-1}{\rho}\nabla p+g(\alpha T+\alpha_C C)\hat{\imath}+\frac{1}{\rho}\nabla\cdot\tau, \quad (1)$$

conservation of mass is,

$$\nabla\cdot v=0, \quad (2)$$

conservation of energy is,

$$\left(\frac{\partial}{\partial t}+v\cdot\nabla\right)T=\kappa\nabla^2 T, \quad (3)$$

and the conservation of composition is,

$$\left(\frac{\partial}{\partial t}+v\cdot\nabla\right)C=D\nabla^2 C. \quad (4)$$

In these equations t is time, $v[v(u, v, w)]$ velocity, ρ the mean density, p is pressure, T is temperature, C is the concentration of the light component in the binary magma, κ is the thermal diffusivity, and D is the chemical diffusivity of the light component. $\hat{\imath}$ is the unit vector in the Z (downward vertical) direction. The viscous stress tensor, τ, for a Newtonian fluid is given by:

$$\tau_{ij}=\eta\left(\frac{\partial v_i}{\partial X_j}+\frac{\partial v_j}{\partial X_i}\right), \quad (5)$$

where the viscosity, η, is given by:

$$\eta(\bar{T})=\eta_0\exp(-A\bar{T}), \quad (6)$$

where A is a constant and η_0 is a reference viscosity. $\bar{T}$ is a dimensionless temperature and is defined shortly. The coefficients of thermal expansion and its analogous compositional counterpart are given by:

$$\alpha\equiv\frac{-1}{\rho}\left(\frac{\partial\rho}{\partial T}\right)_{\mathrm{C,p}} \quad \text{and} \quad \alpha_{\mathrm{C}}\equiv\frac{-1}{\rho}\left(\frac{\partial\rho}{\partial C}\right)_{\mathrm{T,p}}. \quad (7)$$

Equations (1–4) are made dimensionless by choosing $\bar{Z}=Z/d$, $\bar{t}=t\kappa/d^2$, $\bar{p}=pd^2/\rho\nu\kappa$, $\bar{T}=(T-T_0)/\Delta T$ and $\bar{C}=(C-C_1)/\Delta C$ where d is the depth of the chamber, T_0, T_1, C_0 and C_1 the temperature and mass fraction of light component at the top and bottom of the chamber, respectively and $\Delta T=T_1-T_0$ and $\Delta C=C_0-C_1$.

Following the work of HERRING (1963, 1964), GOUGH *et al.* (1975) and TOOMRE *et al.* (1977), the single-mode mean field approximation is used to simplify Equations (1) through (4). The dimensionless vertical velocity ($\bar{w}$), temperature ($\bar{T}$) and composition ($\bar{C}$) are decomposed according to:

$$\bar{w}=\tilde{W}(\bar{Z},\bar{t})f(\bar{X},\bar{Y}) \quad (8a)$$

$$\bar{T}=\tilde{T}(\bar{Z},\bar{t})+\theta(\bar{Z},\bar{t})f(\bar{X},\bar{Y}) \quad (8b)$$

$$\bar{C}=\tilde{C}(\bar{Z},\bar{t})+\phi(\bar{Z},\bar{t})f(\bar{X},\bar{Y}). \quad (8c)$$

The first term in Equations (8b) and (8c) is a non-fluctuating component which varies solely in $\bar{Z}$ and $\bar{t}$. This non-fluctuating component is the horizontal average of the quantity. In an arrangement of convection cells in which there are as many upwelling as downwelling plumes the horizontal average of $\bar{w}$ is zero and those of $\bar{T}$ and $\bar{C}$ non-zero. The second component is the fluctuating component. This component has a magnitude, which is solely a function of $\bar{Z}$ and $\bar{t}$, and which is multiplied by the periodic function $f(\bar{X}, \bar{Y})$. This function represents the convective planform and wavelength. In the case of convection cells in the form of infinitely long rolls $f(\bar{X}, \bar{Y})$ has the form cos $k\bar{X}$. The reader is referred to SEGAL and STUART (1962) and GOUGH *et al.* (1975) for further discussion of the form of $f(\bar{X}, \bar{Y})$. The velocity vector, v, has the components:

$$v=\frac{1}{k^2}\frac{\partial f}{\partial X}\frac{\partial W}{\partial Z},\frac{1}{k^2}\frac{\partial f}{\partial Y}\frac{\partial W}{\partial Z},f(X,Y)W(Z,t), \quad (8d)$$

in terms of the mean field formulation. In Equation (8d) and subsequent expressions all parameters are dimensionless unless otherwise stated and tildes have been dropped from the mean quantities $\tilde{W}$, $\tilde{T}$ and $\tilde{C}$.

The equation of motion becomes:

$$\frac{1}{\mathrm{Pr}}\left(\frac{\partial}{\partial t}-D\right)DW+\frac{F}{\mathrm{Pr}}(2W'DW+WDW')$$
$$+\frac{2\eta'}{\eta}\left(W'''-k^2W'+\frac{\eta''}{\eta}W''+k^2W\right)$$
$$=-\mathrm{k}^2(\mathrm{Ra}\theta+Rc\phi), \quad (9)$$

the mean thermal and mean compositional equations are:

$$\frac{\partial T}{\partial t}+(W\theta)'=T'' \quad (10)$$

$$\frac{\partial C}{\partial t}+\mathrm{Le}\,(W\phi)'=C'' \quad (11)$$

and the fluctuating thermal and compositional equations are:

$$\left(\frac{\partial}{\partial t}-D\right)\theta+F(2W\theta'+\theta W')=-T'W \tag{12}$$

$$\left(\frac{\partial}{\partial t}-D\right)\theta+F(2W\phi'+\phi W')=-\mathrm{Le}\,C'W. \tag{13}$$

The operator D used here is defined as:

$$D\equiv\frac{\partial^2}{\partial Z^2}-k^2. \tag{14}$$

In the above equations, a prime indicates partial differentiation with respect to Z. Five dimensionless numbers occur in this set of equations including the Prandtl number (Pr), the Lewis number (Le), the thermal Rayleigh number (Ra), the compositional Rayleigh number (Rc), and the viscosity ratio (Λ) (see Table 2). The kinematic viscosity (ν_0) is defined according to $\nu_0 = \eta_0/\rho$. The Prandtl and Lewis numbers are the ratios of diffusivities and therefore depend solely on magma properties. The two Rayleigh numbers also depend on the external parameters of the problem, namely the depth of the chamber and the compositional and temperature contrasts across it. It is also convenient to define the buoyancy ratio $R\rho \equiv Rc/\mathrm{Ra} = \alpha_C\Delta C/\alpha\Delta T$. The other parameters are k, the horizontal wavenumber and F, a planform constant, which is related to $f(X, Y)$. For rolls and rectangular planforms $F = 0$ whereas for hexagons $F = 1/\sqrt{6}$ (GOUGH *et al.*, 1975). k is related to the cell aspect ratio, a (width to depth), by $k = \pi/a$.

Configuration and boundary conditions

The magma chamber is considered to be infinite in the horizontal direction and bounded, top and bottom, by no-slip horizontal surfaces which have fixed temperature and composition. The no-slip condition at the boundaries ($u = w = 0$) implies that both W and W' are zero. We choose to model a chamber of cool, light silicic magma underlain by hotter, denser mafic magma. These boundary conditions are:

$$W=W'=T=\theta=C-1=\phi=0 \quad \text{at} \quad Z=0\ \text{(top)} \quad \text{and}$$

$$W=W'=T-1=\theta=C=\phi=0 \quad \text{at} \quad Z=1\ \text{(base)}$$

where C represents the mass fraction of the light silicic component. This configuration is that of classical Rayleigh–Bernard convection and as such takes no account of the effects at sidewalls.

It should be noted that the specification of T and C at the boundaries implies an unknown flux of heat and composition respectively. The boundaries of the chamber can be considered as infinite thermal and compositional reservoirs. The two implied fluxes are an output of the model and can be tested against geological observations. Alternatively, one could specify the gradients of T or C, or both, at the boundaries and solve for the distribution of T and C.

The model also requires specification of a planform and wavelength. Our experiments have been carried out for hexagonal, roll and rectangular planforms. The majority of the experiments have been performed at a wavenumber of π. The π is

Table 2. Important dimensionless numbers

Dimensionless number		Value	Magma chamber range	
Prandtl Number	Pr	ν/κ	10^4–10^8	Ratio of viscosity to thermal diffusivity
Lewis Number	Le	κ/D	10^4–10^{13}	Ratio of thermal to compositional diffusivity
Rayleigh Number	Ra	$\alpha g d^3\Delta T/\kappa\nu$	10^9–10^{17}	Ratio of thermal buoyancy to viscous forces
Compositional Rayleigh Number	Rc	$\alpha_C g d^3\Delta C/\kappa\nu$	See $R\rho$	Ratio of compositional buoyancy to viscous forces
Buoyancy Ratio	$R\rho$	$\alpha_C\Delta C/\alpha\Delta T$	0–100	Ratio of Rc to Ra
Viscosity Contrast	Λ	e^{Λ}	1–10^8	Ratio of maximum to minimum magma chamber viscosities

close to the critical wave number for the onset of convection as described by linear stability analysis (BAINES and GILL, 1969; VERONIS, 1965). However, a series of experiments was conducted in which k was varied extensively.

The computer program employed an adaptive finite difference grid with up to 400 points to solve discretized versions of Equations (9–13) (PEREYRA, 1978). In cases where a single steady state solution exists this solution can be arrived at regardless of initial profiles.

RESULTS

Isoviscous, steady-state, infinite Prandtl number convection

When Equation (9) is rewritten for infinite Prandtl number, constant viscosity, steady state convection it becomes much simpler. Additionally, if we choose to model convection rolls or a rectangular convection planform, Equations (12) and (13) lose their dependence on the planform constant (F). It is noted that in the infinite Prandtl number case the momentum equation has no dependence on F. The work here was carried out at a wavenumber (k) of π. After having made these assumptions, the principle variables in the problem are the Lewis number and the compositional and thermal Rayleigh numbers. Given these parameters one solves for W, T, θ, C and ϕ as functions of Z, depth in the chamber. In this work three kinds of results can be distinguished.

(1) For low Rayleigh numbers the steady state solution to the problem is a conductive solution. In this case W, θ and ϕ are all zero, $T = Z$ and $C = 1 - Z$.

(2) A second class of results is characterized by the lack of a solution to the steady state problem. HUPPERT and MOORE (1976) noted the existence of oscillatory and aperiodic solutions to the double-diffusive convection equations for certain conditions. There have been many studies of simplified versions of the equations governing the time dependence of double-diffusive convection. These studies (KNOBLOCH and PROCTOR, 1981; DA COSTA *et al.*, 1981; MOORE *et al.*, 1983; KNOBLOCH *et al.*, 1986; GOLLUB and BENSON, 1980) have intrinsic relevance to the fluid dynamics of turbulence and chaos, and to bifurcation theory.

(3) The third class of results is that of a convective steady state. All such solutions have a velocity profile with depth that has just one maximum. These are single convection cells. Figure 2 shows the W, T, θ, C and ϕ profiles as an example of this class of solutions. The temperature and composition profiles are both characterized by thin boundary layers and isothermal/isochemical cores in the center of the cell. From these solutions, one can calculate rates of heat transfer and chemical transport and investigate the dependence of these rates on Le, Ra and $R\rho$.

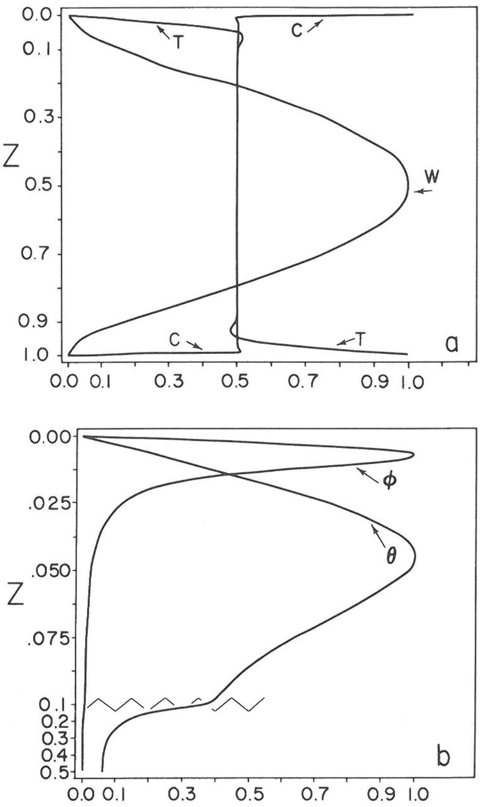

FIG. 2. Representative fields of T, C, W, θ, and ϕ for steady, single-layer, isoviscous, doubly-diffusive systems. Parameters are Le = 300, Ra = 10^7, $R\rho = 25$, $k = \pi$ and Pr $\rightarrow \infty$. (a) Mean temperature (T), mean composition (C) and normalized velocity (W/W_0). $W_0 = 1190$. Computed Nusselt numbers are $\mathrm{Nu_T} = 12.5$ and $\mathrm{Nu_c} = 70.9$. (b) Fluctuating temperature (θ/θ_0) and composition (ϕ/ϕ_0) for same parameters as (a). $\theta_0 = 0.167$ and $\phi_0 = 0.456$.

Steady state, isoviscous, infinite Prandtl number numerical experiments have been conducted over the range $1 \leqslant \mathrm{Le} \leqslant 10^6$, $10^3 \leqslant \mathrm{Ra} \leqslant 10^{10}$, $0 \leqslant R\rho \leqslant 40$ and $k = \pi$. One of the important contributions of this study is the mapping in Le–$R\rho$–Ra space of the region of steady state solutions. The results of almost 300 experiments are displayed in Figure 3. Two fields are distinguished in this figure. The uppermost field is that region of parameter space characterized by the class (3), steady convective solutions. In all cases these solutions are single-layer

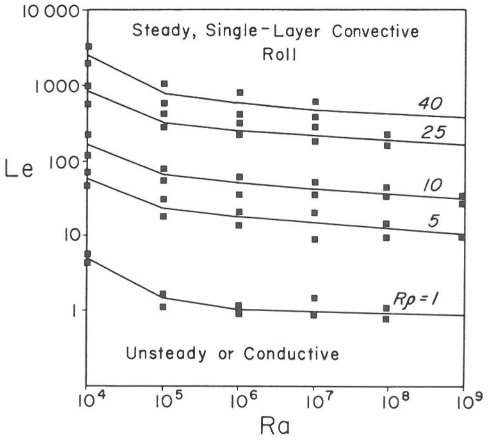

FIG. 3. Regime diagram in the Le–Ra plane separating regions of steady, single-layer, isoviscous roll convection from those characterized by either unsteady convection or conduction profiles ($k = \pi$). At given $R\rho$, Le–Ra values above the curve lead to steady, single-layer solutions characterized by thin thermal and very thin chemical boundary layers. Note that virtually all magma reservoirs with Ra > 10^{10} and Le > 10^4 will be in the steady, single-layer mode even at quite large ratios of chemical to thermal buoyancy ($R\rho$).

convective cells. The lowermost field is made up of both the class (1), conductive, and class (2), unsteady, solutions. A critical Lewis number is defined above for which all solutions are steady convective solutions. It is important to note that this critical Lewis number decreases as the Rayleigh number increases. This is important because magma chambers typically have Rayleigh numbers in excess of 10^9. The critical Lewis number, as determined by a least-squares fit to the data, is given by:

$$\mathrm{Le}_{\mathrm{crit}} = 6.7\ \mathrm{Ra}^{-0.12} R\rho^{5/3}. \qquad (15)$$

The uncertainty in the exponents of this power-law relationship does not exceed ±10%.

Fluxes

The vigor of convection can be measured by the rate at which heat is transferred. The Nusselt number is the ratio of the total heat flux to that which would be carried by conduction alone given the imposed ΔT. Nusselt numbers of unity indicate pure conduction. In the mean field formulation the thermal Nusselt number (Nu_T) and the analogous compositional Nusselt number (Nu_C) are calculated by:

$$\mathrm{Nu}_\mathrm{T} = \frac{\partial T}{\partial Z} - W\theta, \qquad (16)$$

and

$$\mathrm{Nu}_\mathrm{C} = -\left(\frac{\partial C}{\partial Z} - \mathrm{Le}\,(W\theta)\right). \qquad (17)$$

Thermal Nusselt numbers have been calculated for all of the steady convective solutions [class (3)] and these data are plotted on Figure 4. Figure 4a shows the relationship between Nu_T and Ra. It is seen that at high Rayleigh numbers (*i.e.*, $>10^6$) the relationship is linear in log–log space. When plotted against Lewis number (Figure 4b) it can be seen that for high Lewis numbers the thermal Nusselt number is almost independent of Lewis number. This relationship holds so long as $\mathrm{Le}/\mathrm{Le}_{\mathrm{crit}}$ is greater than 10. The $\mathrm{Le}_{\mathrm{crit}}$ is the critical Lewis number for steady convection and given by Equation (15). Thermal Nusselt number is plotted in Figure (4c) versus $R\rho$. When $\mathrm{Le}/\mathrm{Le}_{\mathrm{crit}} > 10$, thermal Nusselt number is almost independent of $R\rho$.

In conclusion, note that Nu_T has little dependence on either Le or $R\rho$. Results of multivariate linear regression are included in Table 3. A simplified equation derived from these results is:

$$\mathrm{Nu}_\mathrm{T} = 0.42\ \mathrm{Ra}^{0.23}. \qquad (18)$$

The uncertainty in the coefficients in Equation (18) and in similar parameterized expressions that follow is about 5%. Physically, this relationship implies that in multicomponent convection heat transport is not affected by the compositional buoyancy of a slow diffusing chemical species. Heat transport is affected only by the magnitude of the thermal driving force and the viscous resistance.

The relationship between heat flux and Rayleigh number can be compared with previous 2–D thermal convection studies. The power-law exponent deduced by the asymptotic solutions of ROBERTS (1979) is 0.2. From the work of LIPPS and SOMERVILLE (1971) at Pr = 200, ROBERTS (1979) calculated the value of the multiplicative coefficient to be 0.426. QUARENI and YUEN (1984) calculated a power law exponent of 0.25. The values of the exponents and coefficients for thermal convection are in reasonable agreement.

In an analogous manner compositional Nusselt numbers have been calculated for the steady convective solutions (Figure 5). Figure 5a indicates a similar relationship to Equation (18) for dependence on Ra. However, the compositional Nusselt number depends also upon the Lewis number (Figure 5b), the power law exponent being about 0.35. Compositional Nusselt number is plotted versus $R\rho$ in Figure 5c. We deduce the following relationship (see also Table 3):

$$\mathrm{Nu}_\mathrm{C} = 0.39\ \mathrm{Ra}^{0.23}\ \mathrm{Le}^{0.35}. \qquad (19)$$

The downward flux of light silicic material depends on both the thermal driving force of the convection and on the ratio of thermal and compositional dif-

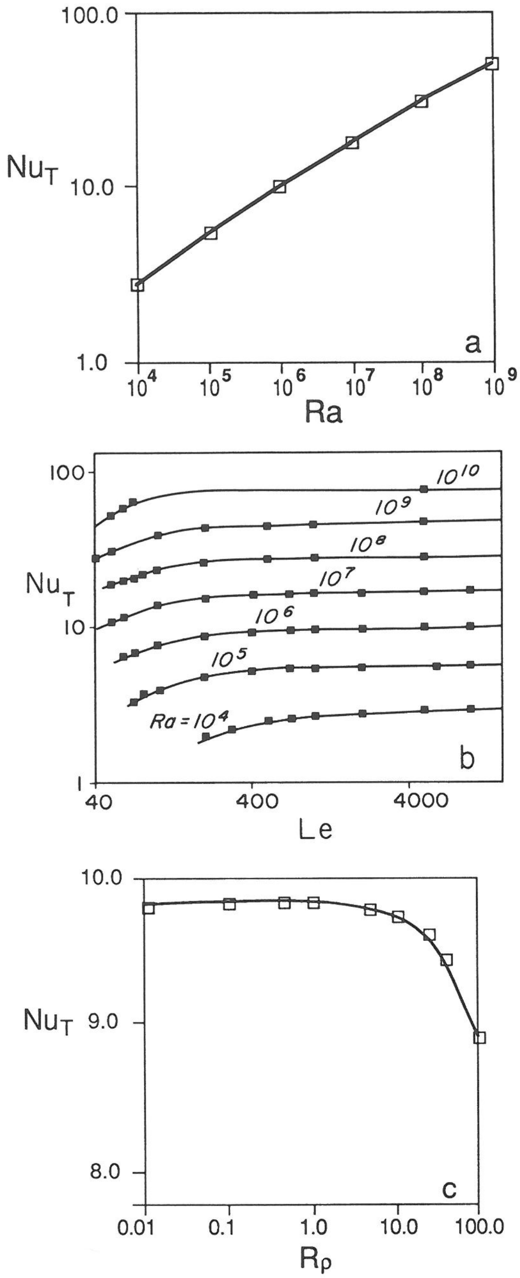

FIG. 4. The relationships between Nu_T and Le, Ra, and $R\rho$ are linear in log–log space away from conditions close to the onset of convection. (a) Log–log relationship between Nu_T and Ra with slope 0.23. Other parameters are Le = 5000, $R\rho = 10$, $k = \pi$. (b) Asymptotic relationship between Nu_T and Le with slope zero. Other parameters are $R\rho = 10$ and $k = \pi$. (c) Nu_T vs. $R\rho$ for Le = 10^4, Ra = 10^6 and $k = \pi$. Slope is close to zero. Dependence of Nu_T on $R\rho$ is weak for $R\rho$ less than a critical value of $R\rho$ (about 10 for the conditions of Figure 4c). Critical values of $R\rho$ depend on Ra [see Equation (15) in text] such that for Ra $\geqslant 10^9$, $(R\rho)_{crit} > 400$. Hence, in the geologically important range, the Le and $R\rho$ dependence of Nu_T is negligible.

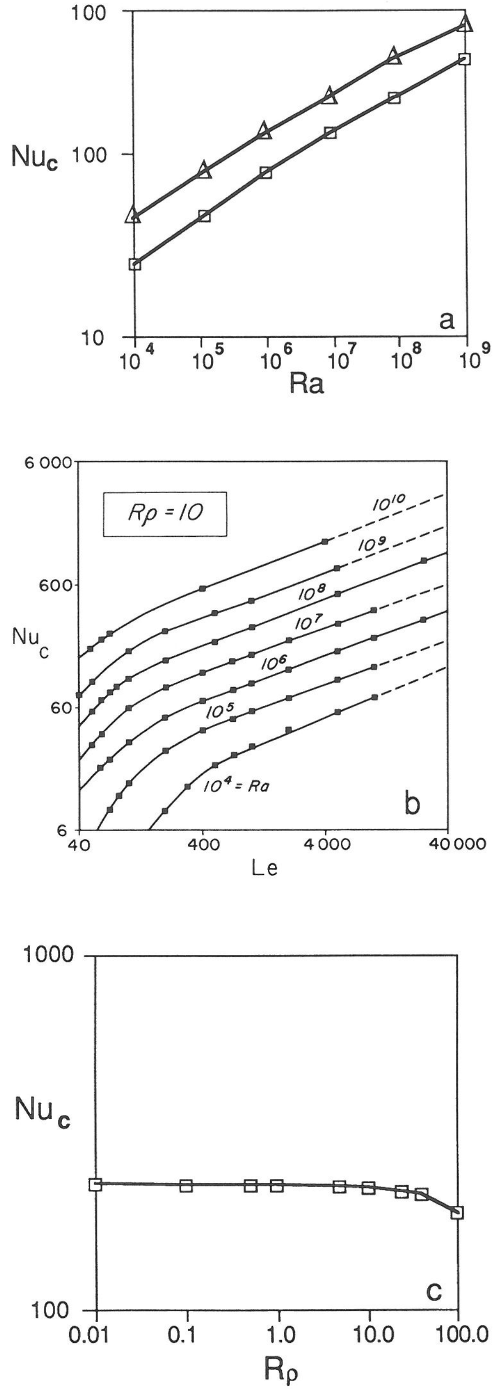

FIG. 5. The relationships between Nu_C and Le, Ra, and $R\rho$ are linear in log–log space away from conditions close to the onset of convection. (a) Log-log relationship between Nu_C and Ra with slope 0.23. Other parameters are Le = 1000 (squares) and 5000 (triangles), $R\rho = 10$, $k = \pi$. (b) Asymptotic relationship between Nu_C and Le with slope 0.35. Other parameters are $R\rho = 10$ and $k = \pi$. (c) Nu_C vs. $R\rho$ for Le = 10^4, Ra = 10^6 and $k = \pi$.

Table 3. Multiple linear regression results for Equations (18) and (19).

	Numerical coefficient	Ra exponent	Le exponent	$R\rho$ exponent
Thermal Nusselt Number Equation (18)	0.417 ± 0.011	0.229 ± 0.001	0.008 ± 0.002	0.009 ± 0.002
Compositional Nusselt Number Equation (19)	0.387 ± 0.010	0.225 ± 0.001	0.345 ± 0.002	0.010 ± 0.002

Correlations include 38 runs and cover the range $10^5 \leqslant \mathrm{Ra} \leqslant 10^9$, $20 \leqslant \mathrm{Le} \leqslant 10^4$ and $0.01 \leqslant R\rho \leqslant 40$.

fusivities. It does not depend on the magnitude of the compositional driving force.

The parameterizations which follow, in addition to the two above, are made for the asymptotic portions of the dataset. These parameterizations therefore imply conditions far into the convective regime, *i.e.*, (high Lewis and Rayleigh numbers) $\mathrm{Le}/\mathrm{Le}_{\mathrm{crit}} > 10$ and $\mathrm{Ra} \geqslant 10^6$.

Velocity

Figure 6 shows the relationship between maximum dimensionless velocity ($W_{\max}$) and Rayleigh number (Ra). At conditions away from the critical parameters for class (3) solutions, the velocity is solely dependent upon thermal Rayleigh number. The following relationship has been deduced from the numerical experiments:

$$W = 0.09\ \mathrm{Ra}^{0.62}. \tag{20}$$

Again comparison can be made to previous thermal convection studies. ROBERTS (1979) found a power-law relationship between Rayleigh number and velocity with an exponent of 0.6. Our results are quite close to this exponent.

Boundary layer thicknesses

The convection cells have narrow thermal and compositional boundary layers of thickness, δ_{T}, and, δ_{C}, respectively. The boundary layer thicknesses are defined by the region in which 95% of the variation in temperature or composition, in one half of the convection cell, takes place. The δ_{T} and δ_{C} vary inversely with Nu_{T} and Nu_{C} respectively. It is found that

$$\delta_{\mathrm{T}} = 0.77 d\ \mathrm{Ra}^{-0.23}, \tag{21}$$

and,

$$\delta_{\mathrm{C}} = 0.77 d\ \mathrm{Ra}^{-0.23}\ \mathrm{Le}^{-0.35}. \tag{22}$$

Note that the ratio of $\delta_{\mathrm{T}}/\delta_{\mathrm{C}}$ is given by:

$$\frac{\delta_T}{\delta_C} = 0.85\ \mathrm{Le}^{0.35}. \tag{23}$$

Finite Prandtl number solutions

A series of numerical experiments was conducted for finite Prandtl number assuming a hexagonal convective planform. Figure 7 shows the variation in thermal Nusselt number as Prandtl number is decreased. There is no dependence of thermal Nusselt number on Prandtl number for values of $\mathrm{Pr} > 10^2$. For $\mathrm{Pr} < 10^2$ the thermal Nusselt number begins to rise quite sharply, indicating increased vigor of convection. Physically, this situation corresponds to an increasing importance of the inertial terms in the momentum equation. Laboratory double–diffusion experiments have been conducted for fluids with Prandtl numbers less than 10. Extrapolation of these laboratory experiments to magma conditions, for which Prandtl numbers exceed 10^2, may be problematical. Future laboratory or numerical experiments are warranted to shed light on this important point.

Effect of wavenumber

The effect of wavenumber on the style of convection has been extensively studied in this work for the conditions $\mathrm{Ra} = 10^6$, $\mathrm{Le} = 500$, $R\rho = 5$, Pr

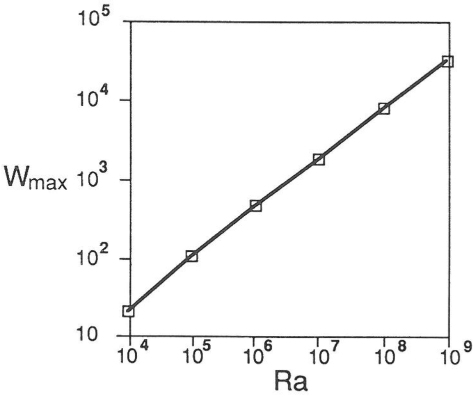

FIG. 6. Log-linear relationship between the maximum velocity, $W_{\max}$, and Ra with slope 0.62. Parameters are $\mathrm{Le} = 1000$, $R\rho = 10$ and $k = \pi$.

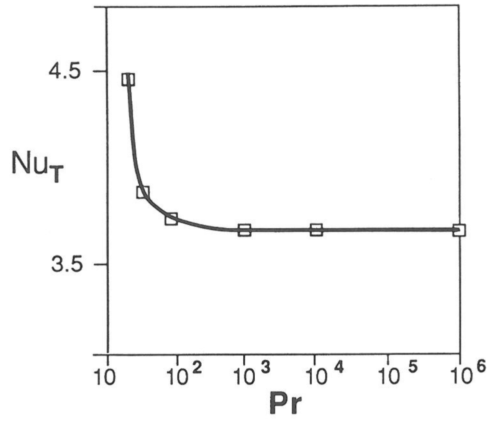

FIG. 7. Variation of thermal Nusselt number, $\mathrm{Nu_T}$ with Prandtl number, Pr. There is no dependence on Pr for Pr $> 10^3$. The other parameters are Le = 100, $R\rho = 10$, Ra $= 10^5$ and $k = \pi$ and the planform chosen is hexagonal. Solutions for Pr < 15 are non-convergent. Note asymptotic limit for Pr > 100.

$= \infty$, and $1 \leqslant k \leqslant 28$ (Figure 8). For $k \geqslant 10$ two branches of steady state solution are found.

The upper branch has a maximum thermal Nusselt number ($\mathrm{Nu_{mx}}$) of 12.8 at wavenumber of 12. This branch of solutions is made up of single convection cells like those illustrated in Figure 2. No solution along this branch could be found for $k > 24$. The lower branch of solutions extends from $k = 10$ to $k = 20$. The solutions along this branch have thermal Nusselt numbers which are roughly half those on the upper branch. The form of these solutions is illustrated in Figure 9. Two vertically stacked convecting layers are separated by a stationary diffusing interface.

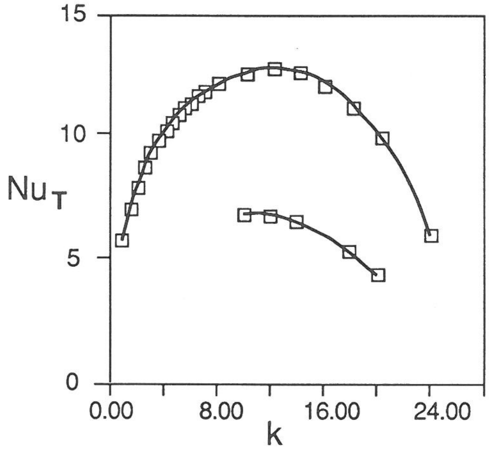

FIG. 8. Variation of thermal Nusselt number, $\mathrm{Nu_T}$, with wavenumber, k, for Le = 500, $R\rho = 5$, Ra $= 10^6$. For $k \geqslant 10$, two sets of solutions can be obtained. The lower branch is a branch of steady double-layer convection cells. The upper branch is one of steady single-layer convection cells.

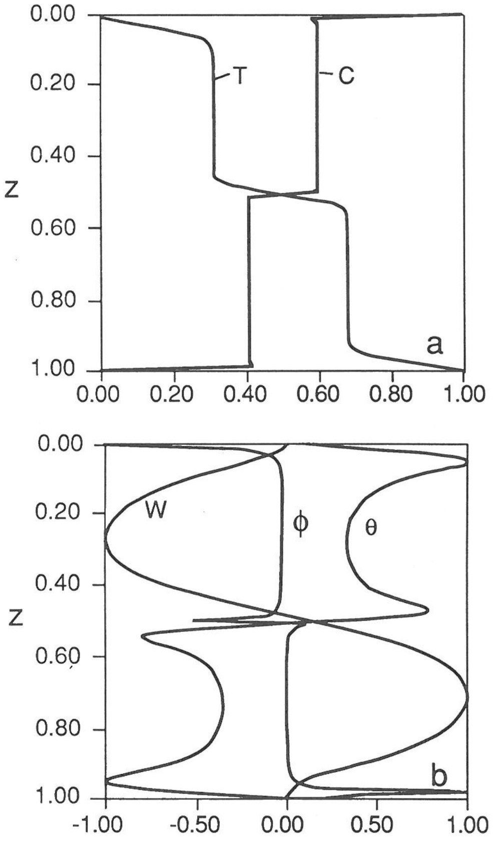

FIG. 9. Representative fields of T, C, W, θ, and ϕ for steady, two-layer, isoviscous, doubly-diffusive systems at high wavenumber. Parameters are Le = 500, Ra $= 10^6$, $R\rho = 5$, $k = 12$ and Pr $\rightarrow \infty$. (a) Mean temperature (T) and mean composition (C) plotted versus depth in the chamber (Z). Computed Nusselt numbers are $\mathrm{Nu_T} = 6.793$ and $\mathrm{Nu_C} = 79.473$. (b) Normalized velocity (W/W_0) (curve W), fluctuating temperature (θ/θ_0) (curve θ) and composition (ϕ/ϕ_0) (curve ϕ) versus depth (Z). $W_0 = 186$, $\theta_0 = 0.105$ and $\phi_0 = 0.021$.

The following remarks can be made about these results.

(1) In cases where two steady state solutions have been found for a fixed set of parameters, the initial profiles determine whether a single or double layer solution is found.

(2) The effect of wavenumber on mean field thermal convection has been studied by TOOMRE *et al.* (1977) and QUARENI and YUEN (1984). Both groups found only single layer solutions. In the present work, pure thermal convection runs were performed for Ra $= 10^6$, Pr $= \infty$ and $1 \leqslant k \leqslant 24$.

The steady state calculation produced single layer results over all of this range given $\theta_{\text{init}} = \phi_{\text{init}} = 0.01$ Sinπz. If, however, the double–layer θ profile from the runs described above was used as the initial guess for the thermal convection case, a fully converged two–layer solution would be found in the range $8 \leqslant k < 20$. The laboratory experiments of J. M. OLSON and ROSENBERGER (1979) reported multi-layer configurations for thermal convection in narrow enclosures. Our mean–field predictions for thermal convection are in good agreement with these experiments and are displayed in Figure 10.

(3) Solutions for $k \geqslant 20$ in the thermal and double diffusive cases along double and single layer solution branches all show non–isothermal cores in convection cells. Composition (in the double diffusive case) still remains isochemical.

(4) TOOMRE *et al.* (1977) note that there is no logical reason for choosing an appropriate wavelength for convection within the mean field formulation. They compared the results of physical experiments to their work and found that the Nusselt number obtained in experiments was typically less than the maximum, Nu_{mx}. This conclusion leaves two choices of wavenumber. TOOMRE *et al.* (1977) suggest that the lower of these two wavelengths is the appropriate one to model convection. They find that numerical modelling of higher wavelengths leads to profiles, such as in (3) above, which are not seen in laboratory experiments. Over the range $10^6 < \text{Ra} < 10^8$ they find that the value of wavenumber (k) that compares best with experimental data lies in the range $1.5 < k < 3$.

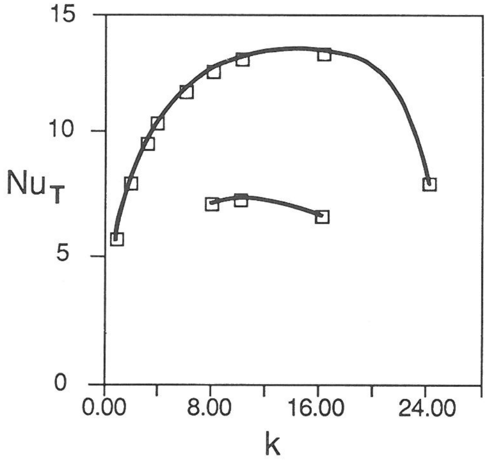

FIG. 10. Variation of thermal Nusselt number, Nu_T, with wavenumber, k, for purely thermal convection and $\text{Ra} = 10^6$. For $k \geqslant 8$ two sets of solutions can be obtained. The upper branch (single layer) can be continued to lower wavenumbers, whereas the lower branch (double layer) cannot.

In modelling steady state double–diffusive convection we have fewer relevant physical experiments with which to compare our data. However, as is illustrated in the above, the qualitative similarity between thermal and double–diffusive convection, with respect to wavenumber, is very strong. On this basis we feel the choice of $k = \pi$ made for the majority of steady state double–diffusive convection runs is an appropriate one.

Effect of variable viscosity

A series of numerical experiments in which viscosity varied as a function of temperature was performed. In Equation (9) this condition results in non–zero values for those terms containing spatial derivatives of viscosity. This result complicates the solution of the momentum equation. In this work we follow QUARENI *et al.* (1985) and make the substitution:

$$Y = \frac{d^3W}{dZ^3} + \frac{1}{\eta}\frac{d\eta}{\partial Z}\left(\frac{d^2W}{dZ^2} + k^2 W\right). \tag{24}$$

Then for infinite Prandtl number Equation (9) becomes:

$$\frac{dY}{dZ} + \frac{1}{\eta}\frac{d\eta}{dZ}\left(Y - 3k^2\frac{dW}{\partial Z} - 2k^2\frac{d^2W}{\partial Z^2}\right) + k^4 W = \frac{-k^2}{\eta}(\text{Ra}\,\theta + Rc\phi). \tag{25}$$

The conditions over which viscosity is included as a variable are $1 \leqslant R\rho \leqslant 10$, $1 \leqslant \text{Le} \leqslant 100$, $10^4 \leqslant \text{Ra} \leqslant 10^7$ and $\text{Pr} = \infty$. The parameter A [equation (6)] is positive in all numerical experiments; therefore, viscosity never exceeds the reference viscosity (η_0). The ratio of maximum and minimum viscosities in the chamber is given by $\Lambda = e^A$. The greatest value of Λ in these experiments was about 600.

Figure 11 presents a comparison between results with $\Lambda = 1$ and $\Lambda \sim 25$ for $R\rho = 5$, $\text{Ra} = 10^6$, $\text{Le} = 100$ and $k = \pi$. High Λ leads to a higher average velocity in the chamber. This conclusion is a direct consequence of the lowered viscosity as temperature increases away from the upper boundary. The velocity field also becomes asymmetric as Λ increases. Slower velocities are present in the upper cooler boundary layer. In the upper boundary layer, diffusional transport is more important, relative to advection, than it is at the lower boundary. For this reason the contrasts in T and C across the upper boundary layer are greater than they are across the lower boundary layer. The differing importance of

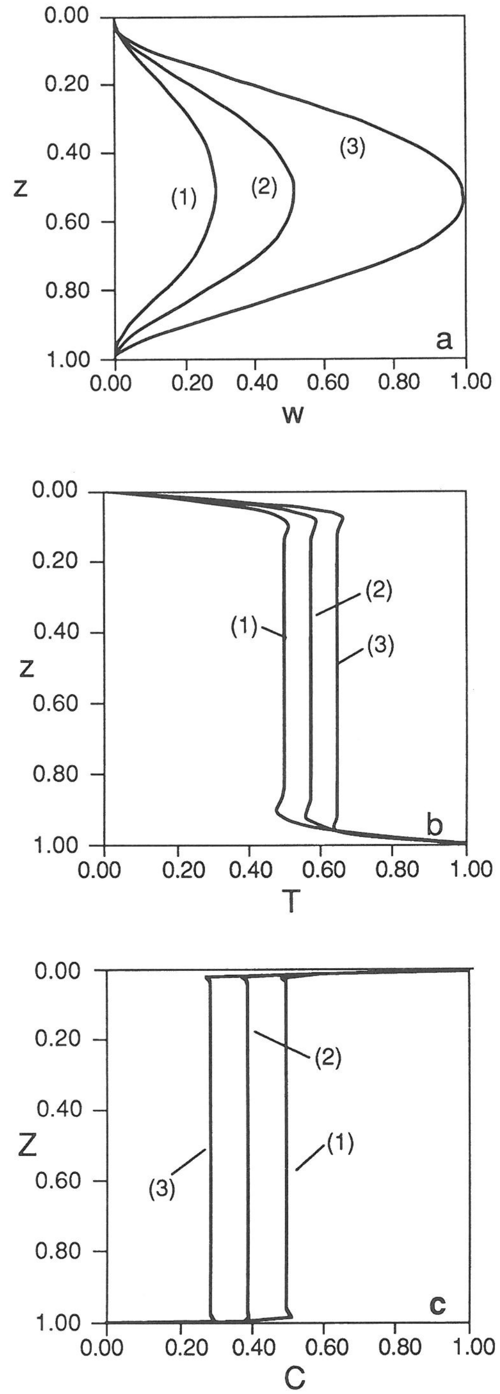

FIG. 11. Representative fields of T, C and W for steady, single-layer, double-diffusive systems with temperature dependent viscosity. Plots are made against depth (Z). Parameters are Le = 100, Ra = 10^6, $R\rho = 5$, $k = \pi$ and Pr $\rightarrow \infty$. In these plots $\Lambda = 0$, 5 and 25 (curves 1, 2, and 3 respectively). (a) Normalized velocity (W/W_0), (b) mean temperature (T) and (c) mean composition (C). $W_0 = 1292$.

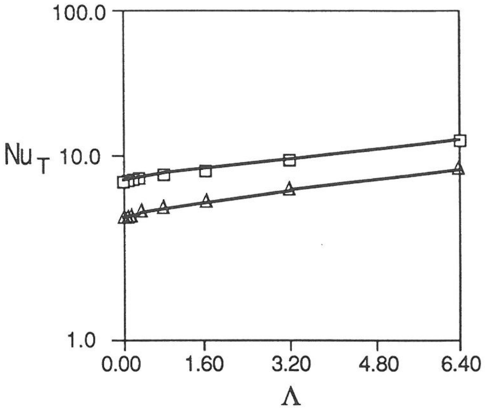

FIG. 12. Log–log relationship between Nu_T and viscosity parameter Λ. Parameterization of Nu_T with leads to the relationship $Nu_T = 0.42\ Ra^{0.23}\Lambda^{0.10}$. Graphs are for Le = 10, Ra = 10^6, $R\rho = 1$ and $k = \pi$ (upper curve), and Le = 100, Ra = 10^5, $R\rho = 1$ and $k = \pi$ (lower curve).

diffusion across the boundary layers accounts for T and C values in the core of the convection cell which differ from 0.5 when Λ is other than unity.

Figure 12 illustrates the dependence of Nu on Λ. Over the range of the experiments a linear fit in log–log space is obtained. Equation (18) then becomes:

$$Nu_T = 0.42\ Ra^{0.23}\Lambda^{0.10}. \tag{26}$$

Nu_C also has a similar relationship with Λ. Equation (19) becomes:

$$Nu_C = 0.39\ Ra^{0.23}\ Le^{0.35}\Lambda^{0.05}. \tag{27}$$

Approximate relationships describing the upper and lower thermal boundary layer thicknesses (δ_{TU} and δ_{TL}, respectively) are given by:

$$\delta_{TU} \approx 0.77\ Ra^{-0.23}\Lambda^{-0.08}, \tag{28}$$

and,

$$\delta_{TL} \approx \delta_{TU}\Lambda^{-0.12}. \tag{29}$$

Similarly, the upper and lower compositional boundary layer thicknesses (δ_{CU} and δ_{CL}, respectively) are given by:

$$\delta_{CU} \approx 0.77\ Ra^{-0.23}\ Le^{-0.35}\Lambda^{-0.04} \tag{30}$$

and,

$$\delta_{CL} \approx \delta_{CU}\Lambda^{-0.22}. \tag{31}$$

GEOLOGICAL IMPLICATIONS

Magma chamber parameters

Appropriate ranges of the governing dimensionless numbers relevant to flow in crustal and upper mantle magma reservoirs are given in Table 2. The specific chemical properties of a given component (*e.g.*, SiO_2, H_2O, MgO, etc.) enter into both the Lewis number (Le) and buoyancy ratio ($R\rho$). Although composition has an obvious effect on viscosity, inertia is of negligible importance in most magmatic flows and the infinite Pr limit is entirely justified *a priori.* Compositional expansivities (α_C) fall between approximately 0.1 and 2 for the major components in a silicate melt; the large value of 2 is associated with H_2O component (see Table 1). Note that the range of $R\rho$ values covered by the numerical experiments corresponds well with those in nature.

Although it is generally assumed that thermal Rayleigh numbers applicable to magma chamber convection are quite large (SHAW, 1965, 1974; BARTLETT, 1969; SPERA, 1980; HARDEE, 1983; SPERA *et al.*, 1982, 1986b), this has recently been questioned (MARSH, 1985). MARSH (1985) argued that the heat transfer through magma chambers, being limited by conductive heat transfer in the country rock, must imply low Rayleigh numbers. The following example demonstrates that the Rayleigh number is large even when heat fluxes are small (*e.g.*, 1 HFU). The simplest way to show this is to envision the heat transfer along a vertical country-rock magma-chamber contact. A uniform heat flux assumed along the boundary is governed by heat conduction in the country rock.

A scaling analysis of the two-dimensional form of the conservation equations of heat and momentum enables one to estimate the thermal boundary layer thickness (δ_T) and the Nusselt number. The analysis gives:

$$\delta_T \sim LR^{-1/5}, \qquad (32)$$

and,

$$\mathrm{Nu}_T = \frac{qL}{\Delta T_1 k_T} \sim \frac{L}{\delta_T} \sim R^{1/5}. \qquad (33)$$

In these expressions, L is the characteristic length of the chamber–country rock contact, ΔT_1 is the temperature difference between chamber interior and wall, q is the heat flux, k_T the thermal conductivity of the country rock (or magma), and R is the Rayleigh number based on the imposed (and constant) heat flux at the chamber wall. The Rayleigh number is defined according to $R = \alpha gqL3/k\kappa\nu$. The validity of these scaling results can be demonstrated by referring to the numerical solution by SPARROW and GREGG (1956), who found:

$$\mathrm{Nu}_T = 0.62R^{1/5}, \qquad (34)$$

in the infinite Prandtl number limit. Application of these results to a magma chamber is made possible once typical parameters are assumed. For illustrative purposes set $L = 1$ km, $\alpha = 5 \times 10^{-5}$ K^{-1}, $g = 10$ m/s^2, $\kappa = 8 \times 10^{-7}$ m^2/s, $k_T = 3.35$ W m^{-1} K^{-1}, $\nu = 10^4$ m^2/s. Choosing a heat flux (q) at the wall of 1 HFU ($=1 \times 10^{-6}$ cal/cm^2 s $= 41.84$ mW/m^2) one finds:

$$R = 8 \times 10^8$$

$$\delta_T \sim 17\,\mathrm{m}$$

$$\Delta T_1 \sim 0.2\,\mathrm{K}.$$

Note that even for the small value of heat flux used here (1 HFU is less than the global average) the implied Rayleigh number is quite large. Even though the temperature difference across the chamber is small, the magma will be actively and vigorously convecting. As is noted below, in many geothermal areas heat flow can be one hundred times greater than the value used here; our estimate of magma chamber Rayleigh number is therefore a low one. On this basis we cannot agree with the findings of MARSH (1985).

Finally, we note that although most of numerical experiments are for Le $\leqslant 10^4$, the asymptotic dependence of Nu_C on Le enables one to estimate light-component transport rates with some degree of confidence. Similarly, the weak dependence of Nu_T on Le and $R\rho$ implies that heat fluxes may be reasonably well calculated even for species characterized by low chemical diffusivities.

The ranges here are valid for a wide variety of magma chamber conditions. The most variable is the Rayleigh number, because of its cubic dependence on length scale. Given these dimensionless numbers it is now possible to apply the results to magma chamber flows. The following calculations use parameterizations which assume a wavenumber (k) of π. This is equivalent to assuming a convection cell as deep as it is wide (*i.e.*, aspect ratio, $a = 1$).

Flux of heat and light–silicic–component

The steady state model fixes temperature and composition at the upper and lower boundaries of the chamber. Such conditions imply fluxes through the boundaries of both heat and the light–silicic component.

Heat flux is a quantity that can be directly compared with measurements made in active geothermal areas, which are presumably underlain by active magma chambers. Unfortunately, uncertainty regarding the present-day size and shape of active magma reservoirs precludes more than a semi-quantitative comparison. For high Lewis number, the thermal Nusselt number is given by Equation (26), so that the dimensional heat flux through the roof of the chamber is given by:

$$q = 0.42 k_T \left(\frac{\Delta T}{d}\right) \mathrm{Ra}^{0.23} \Lambda^{0.10}. \qquad (35)$$

In this equation and in Equations (36) to (39) all quantities are dimensional. For example, with thermal conductivity, $k_T = 3.35$ W m^{-1} K^{-1}, $\Delta T = 5$ K, $d = 5$ km, a magma viscosity of 10^4 Pa·s, $\Lambda = 10^2$ then the heat flux is 3500 mW/m^2 (~80 HFU where 1 HFU = 1×10^{-6} cal/cm^2 s). By allowing for latent heat effects and assuming the hydrothermal system can efficiently dissipate magmatic heat, a hypothetical magma chamber solidification time of roughly 40 000 years may be estimated.

Comparison can be made between the heat fluxes calculated and the heat loss in geothermal areas. Over large geothermal areas (1000 km^2) ELDER (1965) suggests heat flow values averaging 100 HFU (4 200 mW/m^2). More recently, SOREY (1985) has computed the heat discharge divided by caldera area for the Yellowstone, Long Valley and Valles geothermal areas. Heat flux values of 2100, 630 and 500 mW/m^2, respectively, were estimated based on present-day discharge rates of high-chloride thermal water in hot springs and seepage into rivers. It is reassuring that these measurements are in agreement with the numerical experiments.

Rates of transport of silicic–component downward can be calculated from the compositional Nusselt number relationship given by Equation (27). The compositional Nusselt number is defined according to:

$$\mathrm{Nu_C} \equiv \frac{j_i d}{\rho D \Delta C}, \qquad (36)$$

where j_i is the flux of the i^{th} light component, ρ the density, D the chemical diffusivity and ΔC the externally maintained difference in composition across the chamber. By combination of Equations (27) and (33), the dimensional flux of light component is determined according to:

$$j_i = \frac{0.39 \rho \kappa \Delta C}{d} \mathrm{Ra}^{0.23}\, \mathrm{Le}^{-0.65} \Lambda^{0.05}. \qquad (37)$$

With Ra = 8×10^{13}, Le = 10^4 (for water in melt), $\rho = 2500$ kg/m^3, $\kappa = 10^{-6}$ m^2/s, $\Delta C = 0.05$, $\Lambda = 100$ and $d = 5$ km, Equation (34) yields a flux of water, $j_{H_2O} = 5.0 \times 10^{-8}$ kg/m^2 s. If the cross-sectional area of the magma chamber is taken as d^2, then the mass flux corresponds to an effective mass flow rate for H_2O of 4.0×10^7 kg/year. The residence or redistribution time for H_2O within the chamber may be defined as:

$$t_{H_2O} = \frac{C_{H_2O} \rho d}{j_{H_2O}}, \qquad (38)$$

where C_{H_2O} is the average H_2O content of melt within the chamber (say $C_{H_2O} = 0.025$). For the parameters cited, $t_{H_2O} = 2.0 \times 10^5$ years. The effective rate at which H_2O is transported from top to bottom of the chamber is therefore $V_{H_2O} \sim d/t_{H_2O} \sim 2.5$ cm/year. The eddy diffusivity of H_2O corresponding to this rate is roughly D_{eddy} (H_2O) $\sim d^2/t_{H_2O} = 4.0 \times 10^{-6}$ m^2/s which is larger by a factor of 10^5 than the corresponding molecular diffusivity of H_2O of $\sim 10^{-11}$ m^2/s (DELANEY and KARSTEN, 1981; SHAW, 1974). Convection clearly plays a dominant role in the redistribution of H_2O in a magma chamber.

The mass flux can be interpreted in terms of the rate at which crystallization of anhydrous phases takes place at the top boundary of the chamber. In the above example, the implied rate of crystallization of the "upper border group" is $j_i/\rho\Delta C$ which corresponds to about 4 m per thousand years.

Convection rates

From Equation (20), the dimensional maximum convection velocity is given by:

$$W = 0.09 \frac{\kappa}{d} \mathrm{Ra}^{0.62}. \qquad (39)$$

For Ra = 10^{12}, this corresponds to a velocity of 16 km/yr. This value is in agreement with the calculations based on boundary–layer theory made by SPERA *et al.* (1982). The circulation time for a magma parcel is therefore $4d/W \sim 1$ year.

It is noted that both a 5 mm crystal and a 5 cm xenolith will have settling velocities several orders of magnitude less than convective velocities in the center of the cell. This finding suggests that crystal fractionation by settling is very unlikely in melt dominated magma chambers, except at the margins where velocities are smaller. More detailed studies on the distribution of crystals in magma chambers support this finding (MARSH and MAXEY, 1985; WEINSTEIN *et al.*, 1986).

Boundary layer thicknesses

Equations (21) and (22) give the thermal and compositional boundary–layer thicknesses, respectively. For Ra = 10^{12}, Le = 10^4 and $d = 5$ km these boundary layer thicknesses are 6 m and 0.2 m, respectively. Note that δ_C depends on the molecular diffusion coefficient of the light component. Although these calculations do predict that a continuously zoned cap of "evolved" magma will accumulate at the top of a chamber, the thickness of that zone is quite thin.

Existence of layers

Results of numerical experiments plotted in Figure 3 cover a large range of conditions. The values of Prandtl number (Pr) and buoyancy ratio ($R\rho$) in these experiments are in the range of those in magma chambers, *i.e.*, $\mathrm{Pr} = \infty$ and $1 < R\rho < 50$. We are not able to model the complete range of magma chamber Lewis or Rayleigh numbers. However, it is noted that magma chambers lie at Lewis numbers well above the critical Lewis numbers that yield steady single–cell convection. Additionally, as Rayleigh number increases this critical Lewis number will drop even farther from relevant magma chamber Lewis numbers. The data comprising Figure 2 are for $\Lambda = 1$ and $k = \pi$. A primary conclusion of this paper is that given these conditions steady state magma chamber convection cells will be simple single cells. The value of Λ, although changing some of the characteristics of the cells, does not change their single–cell nature.

At values of k greater than 10 (aspect ratio ~ 3) multiple steady states exist. Two points should be noted.

(1) Single and double layer solutions are found for $k \geqslant 10$ in both multicomponent and pure thermal convection experiments. Therefore, they are not solely a phenomena of multicomponent convection.

(2) As we have studied only steady state solutions it is not possible to determine which solution (the single cell or double cell) will be produced in the evolution of a magma chamber. Both solutions should be admitted to be possible in tall, thin magma chambers.

CONCLUSIONS

This study of steady state double–diffusive convection in magma chambers was conducted for boundary conditions which prescribed fixed temperatures and compositions at the top and bottom of the chamber. Within this context, the following conclusions are reached:

(1) The mean–field approximation to the full convective equations can successfully model convection over a large range of magma chamber conditions. In particular it has been possible to model Rayleigh numbers as high as 10^{10} and Lewis numbers as high as 10^5.

(2) Isoviscous convection dominated by a wavenumber of π (as might be expected in an equidimensional magma chamber) is found to exist above a critical Lewis number. Below the critical Lewis number, unsteady and conductive solutions are found. Above the critical Lewis number, all steady–state solutions are single layer convection cells. No layered convection is found. The critical Lewis number is a function of the buoyancy ratio and the Rayleigh number. Magma chambers lie above this critical Lewis number and therefore it is suggested that steady–state magma chambers will exhibit single cell convection.

(3) Convection is characterized by thin thermal boundary layers and thinner compositional boundary layers. The cores of the convection cells are isothermal/isochemical. For the typical parameters used in the text thermal and compositional boundary layer thicknesses are 6 m and 20 cm respectively.

(4) Calculated heat fluxes for magma chambers are in agreement with measured heat fluxes in hydrothermal areas. Such fluxes are of the order of 4200 $\mathrm{mW/m^2}$ (100 HFU).

(5) The boundary conditions imply fluxes of chemical species. For the parameters given in the text, the effective rate at which water is transported through a magma chamber is about 2.5 cm/yr. Evidently convection plays a dominant role in the redistribution of water in magma chambers.

(6) Characteristic convective velocities on the order of km/yr prohibit fractionation by crystal settling in both rhyolitic and basaltic magmas, except within flow along chamber margins.

(7) For hexagonal convection planforms at wavenumber $k = \pi$, the characteristics of the flow become dependent on Prandtl number (Pr) for $\mathrm{Pr} \leqslant 100$. As Prandtl numbers for magmatic systems exceed 100, future work is needed to investigate the nature of this potentially important transition. This dependence is manifested in increased fluxes of heat and composition.

(8) When viscosity is temperature dependent the style of convection is similar to that for isoviscous convection. Velocities and boundary layer thicknesses differ quantitatively from those found in isoviscous convection.

(9) In chambers dominated by high wavenumbers ($k > 10$, such as might be expected in tall thin magma chambers) two steady–state solutions are found. The first, corresponding to a high heat flow, is a single convection cell. The second, corresponding to a low heat flow, consists of two vertically stacked convecting cells separated by a diffusive interface. Given the same parameters and a high wavenumber, both sets of solutions are found for purely thermal convection, in addition to double diffusive convection. It is possible that these double-layer convection cells could occur in tall thin magma chambers. This model, on account of its

steady-state nature, cannot discriminate between these two solutions.

Acknowledgements—This research was supported by NSF EAR85-19900, NSF EAR86-08284 to FJS and NSF EAR86-08479 to DAY. Numerical calculations were supported by the National Center for Atmospheric Research at Boulder, Colorado, the Princeton University Computer Center, the IBM Los Angeles Scientific Computing Center and the offices of the Vice Chancellor and Provost of the University of California at Santa Barbara. We thank Ulli Hansen, Peter M. Olson, Alain Trial, and Curtis Oldenburg for stimulating discussions.

REFERENCES

BACON C. R. (1983) Eruptive history of Mount Mazama and Crater Lake Caldera, Cascade Range, USA. *J. Volcanol. Geotherm. Res.* **18,** 57–115.

BAINES P. G. and GILL A. E. (1969) On thermohaline convection with linear gradients. *J. Fluid Mech.* **37,** 289–306.

BARTLETT R. W. (1969) Magma convection, temperature distribution, and differentiation. *Amer. J. Sci.* **267,** 1067–1082.

BRANDEIS G. and JAUPART C. (1986) On the interaction between convection and crystallization in cooling magma chambers. *Earth Planet. Sci. Lett.* **77,** 345–361.

BOTTINGA Y., WEILL D. F. and RICHET P. (1982) Density calculations for silicate liquids. I. Revised method for aluminosilicate compositions. *Geochim. Cosmochim. Acta* **46,** 909–917.

BURNHAM C. W. and DAVIS N. F. (1971) The role of H_2O in silicate melts, I. *P–V–T* relations in the system $NaAlSi_3O_8$–H_2O to 10 kilobars and 1000°C. *Amer. J. Sci.* **270,** 54–79.

CHEN C. F. and TURNER J. S. (1980) Crystallization in a double-diffusive convection system. *J. Geophys. Res.* **85,** 2573–2593.

CHEN C. F. and JOHNSON D. H. (1984) Double-diffusive convection: a report on an engineering foundation conference. *J. Fluid Mech.* **138,** 405–416.

CRISP J. A. (1984) The Mogan and Fataga formations of Gran Canaria (Canary Islands). Geochemistry, petrology and compositional zonation of the pyroclastic and lava flows; intensive thermodynamic variables within the magma chambers; and the depositional history of pyroclastic flow *E/ET.* Ph.D. Thesis, Princeton Univ.

CRISP J. C. and SPERA F. J. (1986) Pyroclastic flows and lavas from Tejeda volcano, Gran Canaria, Canary Islands: Mineral chemistry, intensive parameters and magma chamber evolution. *Contrib. Mineral. Petrol.* (Submitted).

DA COSTA L. N., KNOBLOCH E. and WEISS N. O. (1981) Oscillations in double-diffusive convection. *J. Fluid Mech.* **109,** 25–43.

DELANEY J. R. and KARSTEN J. L. (1981) Ion microprobe studies of water in silicate melts: concentration-dependent water diffusion in obsidian. *Earth Planet. Sci. Lett.* **52,** 191–202.

ELDER J. W. (1965) Physical processes in geothermal areas. In *Terrestrial Heat Flow,* (ed. W. H. K. LEE), Amer. Geophys. Union Monograph Series No. 8, 211–239.

ELDER J. W. (1969) Numerical experiments with thermohaline convection. *Phys. Fluids,* suppl. II, 194–197.

GOLLUB J. P. and BENSON S. V. (1980) Many routes to turbulent convection. *J. Fluid Mech.* **100,** 449–470.

GOUGH D. O., SPIEGEL E. A. and TOOMRE J. (1975) Modal equations for cellular convection. *J. Fluid Mech.* **68,** 695–719.

GOUGH D. O. and TOOMRE J. (1982) Single-mode theory of diffusive layer in thermohaline convection. *J. Fluid Mech.* **125,** 75–97.

GREER J. C. (1986) Dynamics of withdrawal from stratified magma chambers. M.S. Thesis, Arizona State Univ.

HANSEN U. S. (1986) Zeitabhangige Phaenomenon in thermische und doppelt diffusiver Konvection. Ph.D. Thesis, University of Cologne, West Germany.

HANSEN U. and YUEN D. A. (1985) Two dimensional double-diffusive convection at high Lewis numbers: applications to magma chambers. *Trans. Amer. Geophys. Union* **66,** no. 46, p. 1124.

HARDEE H. C. (1983) Convective transport in crustal magma bodies. *J. Volcanol. Geotherm. Res.* **19,** 45–72.

HERRING J. R. (1963) Investigation of problems in thermal convection. *J. Atmos. Sci.* **20,** 325–338.

HERRING J. R. (1964) Investigations of problems in thermal convection: rigid boundaries. *J. Atmos. Sci.* **21,** 277–290.

HILDRETH W. (1981) Gradients in silicic magma chambers: implications for lithospheric magmatism. *J. Geophys. Res.* **86,** 10153–10193.

HUPPERT H. E. and MOORE D. R. (1976) Non-linear double-diffusive convection. *J. Fluid Mech.* **78,** 821–854.

HUPPERT H. E. and SPARKS R. J. (1984) Double-diffusive convection due to crystallization in magmas. *Ann. Rev. Earth Planet Sci.* **12,** 11–37.

IYER H. M. (1984) Geophysical evidence for the location, shapes and sizes, and internal structures of magma chambers beneath regions of Quaternary volcanism. *Phil. Trans. Roy. Soc. London* **A310,** 473–510.

JAUPART C., BRANDEIS G. and ALLEGRE C. J. (1984) Stagnant layer at the bottom of convecting magma chambers. *Nature* **308,** 535–538.

KNOBLOCH E. and PROCTOR M. R. E. (1981) Nonlinear periodic convection in double-diffusive systems. *J. Fluid Mech.* **108,** 291–316.

KNOBLOCH E., MOORE D. R., TOOMRE J. and WEISS N. O. (1986) Transitions to chaos in two-dimensional double-diffusive convection. *J. Fluid Mech.* **166,** 409–448.

LIPMAN P. W. (1967) Mineral and chemical variations within an ash-flow sheet from Aso caldera, Southwest Japan. *Contrib. Mineral. Petrol.* **16,** 300–327.

LIPPS F. B. and SOMERVILLE R. C. J. (1971) Dynamics of variable wavelength in finite amplitude Bernard convection. *Phys. Fluids* **14,** 759–765.

LOWELL R. P. (1985) Double-diffusive convection in partially molten silicate systems: its role during magma production and in magma chambers. *J. Volcanol. Geotherm. Res.* **26,** 1–24.

MARSH B. D. (1985) Convective regime of crystallizing magmas. *Geol. Soc. Amer. Abstr. Prog.* **17,** 653.

MARSH D. B. and MAXEY M. R. (1985) On the distribution and separation of crystals in convecting magma. *J. Volcanol. Geotherm. Res.* **24,** 95–150.

MCBIRNEY A. R. (1980) Mixing and unmixing of magmas. *J. Volcanol. Geotherm. Res.* **7,** 357–371.

MCKENZIE D. P., ROBERTS J. M. and WEISS N. O. (1974) Convection in the earth's mantle: towards a numerical simulation. *J. Fluid Mech.* **62,** 465–538.

MOORE D. R., TOOMRE J., KNOBLOCH E. and WEISS N. O. (1983) Periodic doubling and chaos in partial differential equations for thermosolutal convection. *Nature* **303,** 663–667.

MURASE T., MCBIRNEY A. R. and MELSON W. G. (1985) Viscosity of the dome of Mount St. Helens. *J. Volcanol. Geotherm. Res.* **24,** 193–204.

NEWELL T. A. (1984) Characteristics of a double–diffusive interface at high density stability ratios. *J. Fluid Mech.* **149,** 385–401.

NILSON R. H. and BAER M. R. (1982) Double diffusive counterbuoyant boundary layer in laminar natural convection. *Int. J. Heat Mass Transfer* **25,** 285–287.

NILSON R. H., MCBIRNEY A. R. and BAKER B. M. (1985) Liquid fractionation. Part II: Fluid dynamics and quantitative implications for magmatic systems. *J. Volcanol. Geotherm. Res.* **24,** 25–54.

OLDENBURG C. M., SPERA F. J., YUEN D. A. and SEWELL G. (1985) Two dimensional double–diffusive convection. *Trans. Amer. Geophys. Union* **66,** no. 46, p. 1124.

OLSON P. (1986) A comparison of heat transfer laws for thermal convection at very high Rayleigh numbers. *Phys. Earth Planet. Int.* (Submitted).

OLSON J. M. and ROSENBERGER F. (1979) Convective instabilities in a closed vertical cylinder heated from below. Part 1. Monocomponent gases. *J. Fluid Mech.* **92,** 609–629.

PEREYRA V. (1978) PASVA3: an adaptive finite difference FORTRAN program for first order nonlinear and ordinary boundary problems. *Lecture Notes Comp. Sci.* **76,** 67–88.

PIASEK S. A. and TOOMRE J. (1980) Nonlinear evolution and structure of salt fingers. In *Marine Turbulence,* (ed. J. C. J. NIHOUL), pp. 193–219. Elsevier.

PROCTOR M. R. E. (1981) Steady subcritical thermohaline convection. J. Fluid Mech. **105,** 507–521.

QUARENI F. and YUEN D. A. (1984) Time–dependent solutions of mean–field equations with applications for mantle convection. *Phys. Earth Planet. Int.* **36,** 337–353.

QUARENI F., YUEN D. A., SEWELL G. and CHRISTENSEN U. R. (1985) High Rayleigh Number convection with strongly variable viscosity: a comparison between mean–field and two–dimensional solutions. *J. Geophys. Res.* **90,** 12633–12644.

RICE A. (1981) Convective fractionation: a mechanism to provide cryptic zoning (macrosegregation), layering, crescumulates, banded tuffs and explosive volcanism in igneous processes. *J. Geophys. Res.* **86,** 405–417.

ROBERTS G. O. (1979) Fast viscous Bernard convection. *Geophys. Astrophys. Fluid Dyn.* **12,** 235–272.

SCHMINCKE H.-U. (1969) Ignimbrite sequence on Gran Canaria. *Bull. Volcanol.* **33,** 1199–1219.

SCHMITT R. W. (1979) The growth rate of supercritical salt fingers. *Deep Sea Res.* **26A,** 23–40.

SCHMITT R. W. (1983) The characteristics of salt fingers in a variety of fluid systems, including stellar interiors, liquid metals, oceans, and magmas. *Phys. Fluids* **26,** 2373–2377.

SEGAL L. A. and STUART J. T. (1962) On the question of preferred mode in cellular thermal convection. *J. Fluid Mech.* **13,** 289–306.

SHAW H. R. (1965) Comments on viscosity, crystal settling and convection in granitic magmas. *Amer. J. Sci.* **263,** 120–152.

SHAW H. R. (1969) Rheology of basalt in the melting range. *J. Petrol.* **10,** 510–535.

SHAW H. R. (1974) Diffusion in granitic liquids: part I, experimental data; part II, mass transfer in magma chambers. In *Geochemical Transport and Kinetics* (eds. A. W. HOFFMAN *et al.*), pp. 139–170. Carnegie Inst. Wash. Publ. 634.

SMITH R. L. (1960) Zones and zonal variations in welded ash–flows. *U.S. Geol. Survey Prof. Paper 354-F,* pp. 149–159.

SMITH R. L. (1979) Ash–flow magmatism. *Geol. Soc. Amer. Special Paper* **180,** pp. 5–27.

SOREY M. L. (1985) Evolution and present state of the hydrothermal system in long valley caldera. *J. Geophys. Res.* **90,** 11219–11228.

SPARROW E. M. and GREGG J. L. (1956) Laminar free convection from a vertical plate with uniform surface heat flux. *Trans. Amer. Soc. Mech. Eng.* **78,** 435–440.

SPERA F. J. (1980) Thermal evolution of plutons: a parameterized approach. *Science* **207,** 299–301.

SPERA F. J., YUEN D. A. and KEMP D. V. (1984) Mass transfer rates along vertical walls in magma chambers and marginal upwelling. *Nature* **310,** 764–767.

SPERA F. J., YUEN D. A. and KIRSCHVINK S. J. (1982) Thermal boundary layer convection in silicic magma chambers: effects of temperature dependent rheology and implications for thermogravitational chemical fractionation. *J. Geophys. Res.* **87,** 8755–8767.

SPERA F. J., YUEN D. A., GREER J. C. and SEWELL G. (1986a) Dynamics of magma withdrawal from stratified magma chambers. *Geology* **14,** 723–726.

SPERA F. J., YUEN D. A., CLARK S. and HONG H.-J. (1986b) Double–diffusive convection in magma chambers: single or multiple layers? *Geophys. Res. Lett.* **13,** 153–156.

TOOMRE J., GOUGH D. O. and SPIEGEL E. A. (1977) Numerical solutions of single–mode convection equations. *J. Fluid Mech.* **79,** 1–31.

TSUYA H. (1955) Geological and petrological studies of Volcano Fuji. *Earth Res. Inst. Bull.* **33,** 341–383. Tokyo Imp. University.

TURCOTTE D. L. and OXBURGH E. R. (1967) Finite amplitude convection cells and continental drift. *J. Fluid Mech.* **28,** 29–42.

TURNER J. S. (1980) A fluid dynamical model of differentiation and layering in magma chambers. *Nature* **285,** 213–215.

TURNER J. S. (1985) Multicomponent convection. *Ann. Rev. Fluid Mech.* **17,** 11–44.

VERONIS G. (1965) On finite amplitude instabilities in thermohaline convection. *J. Marine Res.* **23,** 1–17.

VERONIS G. (1968) Effect of a stabilizing gradient of solute on thermal convection. *J. Fluid Mech.* **34,** 315–336.

WEINSTEIN S. A., YUEN D. A. and OLSON P. (1986) Evolution of crystal–settling in magma–chamber convection. *Earth Planet. Sci. Lett.,* (Submitted).

WILLIAMS H. (1942) The geology of Crater Lake National Park, Oregon, with a reconnaissance of the Cascade Range southward to Mount Shasta. *Carnegie Inst. Wash. Publ. 540,* 162 pp.